

Design Optimization of Ball Grid Array Packaging by the Taguchi Method

Yeong K. Kim[†], Jae-chang Kim and Joo Ho Choi

School of Aerospace and Mechanical Engineering, Korea Aerospace University, 100 Hanggongdae-gil,
Hwajeon-dong, Deogyang-gu Goyang-city, Gyeonggi-do 412-791, Korea

(Received December 6, 2010: Accepted December 20, 2010)

Abstract: In this paper, a design optimization of ball grid array packaging geometry is studied based on the Taguchi method, which allowed robust design by considering the variance of the input parameters during the optimization process. Molding compound and substrate were modeled as viscoelastic, and finite element analyses were performed to calculate the strain energy densities of the eutectic solder balls. Six quality factors of the dimensions of the packaging geometry were chosen as control factors. After performing noise experiments to determine the dominant factors, main experiments were conducted to find the optimum packaging geometry. Then the strain energy densities between the original and optimized geometries were compared. It was found that the effects of the packaging geometry on the solder ball reliability were significant, and more than 40% of the strain energy density was reduced by the geometry optimization.

Keywords: Reliability, Optimization, Viscoelasticity, Taguchi method

1. Introduction

The progress toward the compactness of modern microelectronics devices faces numerous challenges in various engineering areas. Among these, thermal and mechanical reliability has been a primary issue over the last decades. As well known, the mechanical stresses develop due to the heterogeneous nature of the component materials in the packaging structure, which results in behaviors mismatch under environmental changes. For the evaluation of the packaging reliability, experimental methods such as accelerated testing are widely adopted.^{1, 2)} Although the methods are relatively simple and robust, the time and cost for the prototype manufacturing are substantial. In addition, it is not easy to obtain the stress development mechanism, which is essential to improve the packaging structure reliability. To overcome this drawback, numerical simulation has been widely employed to analyze, understand and predict the mechanical failure. However, the prediction of the simulation results are occasionally different from the experimental data, mainly due to inappropriate modeling of mechanical material properties such as elastic assumptions for viscoelastic materials. Comprehensive analyses and discussions on this subject were reported by Kim et al.³⁾ They showed that, in addition to the better results, the viscoelastic calculations provided in-depth insights in understanding the stress development mechanism. They also demonstrated that the elastic calculations

could lead to inappropriate prediction in 'what-if' study. Recently, efforts to enhance the mechanical reliability of solder joints have been extended to optimal geometry design through statistical methods such as design of experiments (DOE) and the Taguchi method.⁴⁻¹⁰⁾ The studies calculated the strain energy densities of the solder balls as quality characteristics, and changed the geometry dimensions of the component material structures. However, all the previous results were based on the elastic approaches where the viscoelastic material properties of the molding compound and the substrate were modeled as elastic.

The objective of this study was to explore a design optimization of the ball grid array packaging structure based on the viscoelastic calculations. The material properties of the molding compound and the substrate were measured and modeled as viscoelastic. Using the data, simulations based on viscoelastic finite element method were performed under accelerated thermal cycles to yield the strain energy densities of the solder balls. The Taguchi method¹¹⁾ was employed for the geometry optimization, and six different dimensions such as the thickness of the materials and solder pitches were considered as quality factors. Strain energy density of the solder ball was employed as objective function. After the optimization, the energy densities of the original packaging and optimized packaging were compared for the evaluation.

[†]Corresponding author

E-mail: yeong.kim@kau.ac.kr

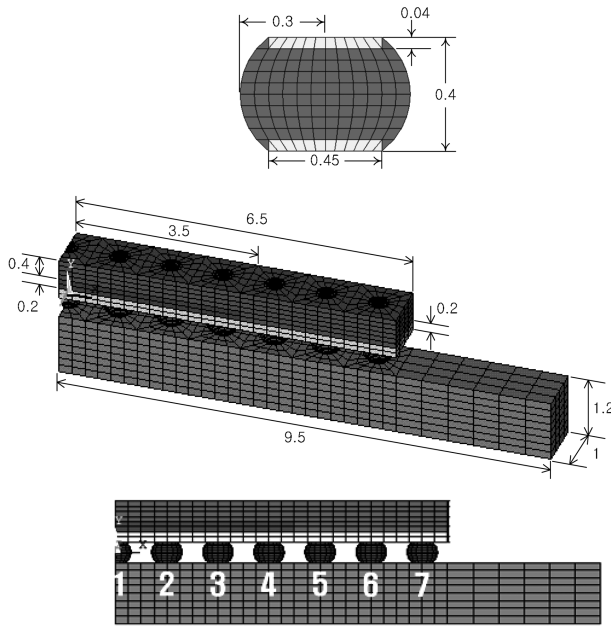


Fig. 1. The geometry and element distribution of the ball grid array package (3D geometric modeling). The solder balls are numbered for their identities. (Unit: mm)

2. Modeling

For the simulation, a typical PBGA packaging structure was modeled as a three dimensional strip. Fig. 1 shows the packaging structure with relevant dimensions. The packaging structure involved molding compound to encapsulate the silicon chip, and thin FR-4 substrate of an epoxy/glass fabric composite material was considered. The viscoelastic material properties were readily measured in the previous work,³⁾ and the results are presented in Fig. 2 and Fig. 3. As seen, the molding compound exhibited strong viscoelastic

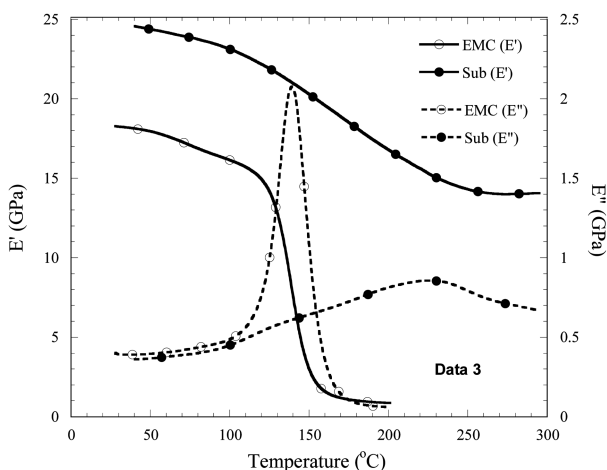


Fig. 2. Dynamic mechanical analysis results of the molding compound and the substrate.

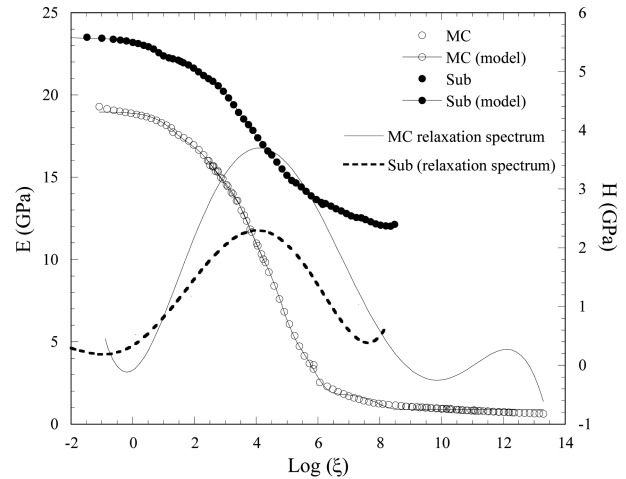


Fig. 3. Mastercurves and relaxation spectrum of the molding compound and substrate.

behavior, and the substrate also showed viscoelastic characteristics, although it was not strong as the molding compound. The glass transition temperatures of the molding compound and the substrate were 105°C and 175°C, respectively. Mastercurves of the materials were also measured by a series of stress relaxation tests based on viscoelastic theory. The data are represented in Fig. 3, where the solid lines represent the moldings by exponential function series (a.k.a. Prony series). And the corresponding shift functions are shown in Fig. 4. The parameters of the mastercurve modelings and the shift functions are listed in Ref. 3. Other mechanical properties such as coefficients of thermal expansion and Poisson's ratios of the molding compound and the substrate, and the elastic properties of the silicon and copper are listed in Table 1. Due to the lack of data, the printed circuit board (PCB) was assumed as elastic for this preliminary study, and also listed in Table 1. To examine the relaxation behavior, relaxation time spectra were calculated using the Alfrey approximation¹²⁾ as

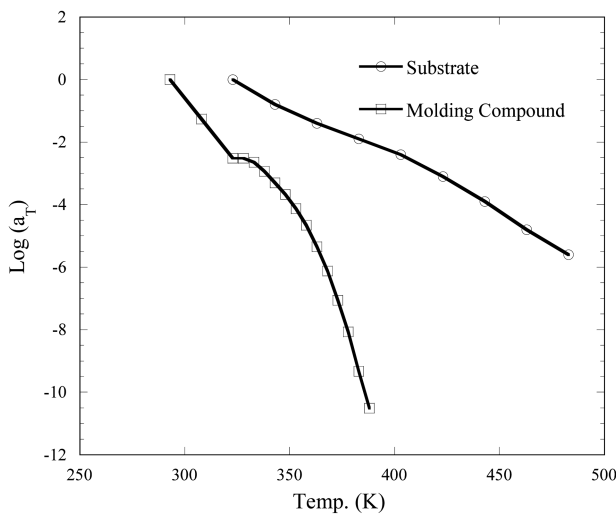
$$H(t) = \left| \frac{d(E(t))}{d(\log(\xi))} \right|_{\xi=t} \quad (1)$$

Equation (1) indicates that the relaxation spectrum can be obtained from the slope of the mastercurve without complex calculations. The results are also plotted in Fig. 3. The peak relaxation times of the molding compound and the substrate are 10^{4.5} minutes and 10^{3.9} minutes, respectively, indicating that the two materials have similar relaxation behaviors.

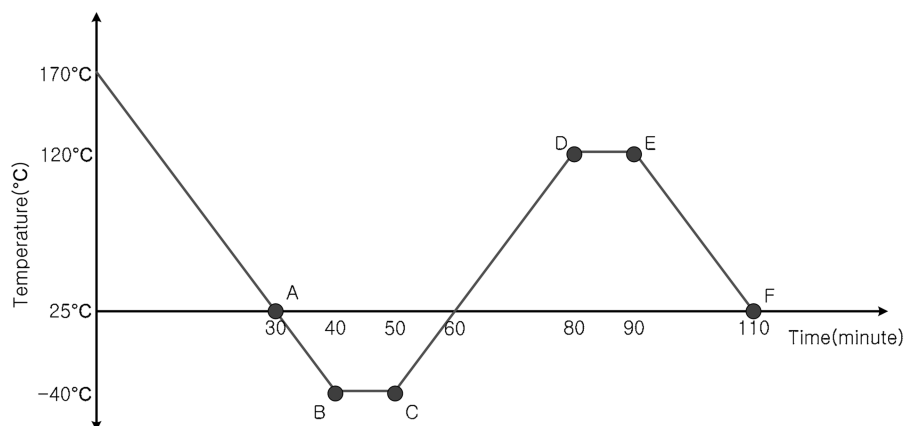
In the simulation, ANSYS (v. 12.1) was used for the strain energy density calculations using solid 185 elements for the entire modeling. The solder balls were assumed as Sn40Pb solder alloy, and Anand's model parameters were

Table 1. Elastic mechanical properties of the component materials of the PBGA packaging structure. MC and Sub represent the molding compound and the substrate, respectively.

	E (GPa)	Poisson's Ratio	CTE (ppm/°C)	T _g
MC		0.26	α_1 : 14.5 α_2 : 56.6	105°C
Sub		0.27	11e-6	175°C
Silicon	160	0.23	2.6e-6	
PCB	22	0.28	12.7e-6	
Cu	130	0.34	17.8e-6	

**Fig. 4.** Shift functions of the molding compound and substrate.

employed for the constitutive equation.¹³⁾ To evaluate the fatigue process, the individual strain energy densities accumulated in the solder balls illustrated in Fig. 1 were calculated. The thermal cycles used for the simulations are shown in Fig. 5. The temperature cooled down from 170°C to room temperature to simulate the molding compound cure, and one more cycle was added after the cooldown.

**Fig. 5.** Temperature cycle profile for strain density calculations.

The cooling and heating rates were about $-5^{\circ}\text{C}/\text{min}$ and $5^{\circ}\text{C}/\text{min}$, respectively. The strain energy densities were calculated during the thermal cycle, and recorded at six different times to trace the energy density accumulations. Fig. 6 shows the strain energy density accumulation profiles for the solder balls. As seen, the energy density increased as the thermal cycle proceeded, and the highest value was found in the solder ball no. 4.

2.1. Optimization

The Taguchi optimization process employed in this study was similar to the work by Lai and Wang.⁶⁾ Six quality control factors and their levels were chosen, as listed in Table 2. All the factors had three levels: Level 2 is the original dimensions, and Level 1 and Level 3 were reduced and increased thicknesses. The Taguchi method was employed to reduce the number of experiments, and L_{27} (3^6) orthogonal array was obtained for the main experiments. The smaller-the-better signal to noise (S/N) was defined as

$$S/N = -10 \log \frac{\sum_{i=1}^r y_i^2}{r} \quad (2)$$

where y_i is the i th measurement data and r is the number of measurements. In this study, the objective function $y \equiv W$ was the accumulated strain energy density of the solder ball at the point F in Fig. 5. In the actual calculations, the numerical results do not contain experimental errors. Therefore, artificial data errors were generated by intentional deviations in the noise experiments by imposing $\pm 4\%$ noise on the control factors. In Table 3, two-level noise factors were implemented in an L_8 (2^6) orthogonal array in which level 1 and level 2 stood for the corresponding noise factor with -4% and $+4\%$ noises, respectively.

Table 4 and Fig. 7 show the responses calculated from the results presented in Table 3. In Table 4, level i of factor j is

Table 2. Control factors and levels (unit: mm).

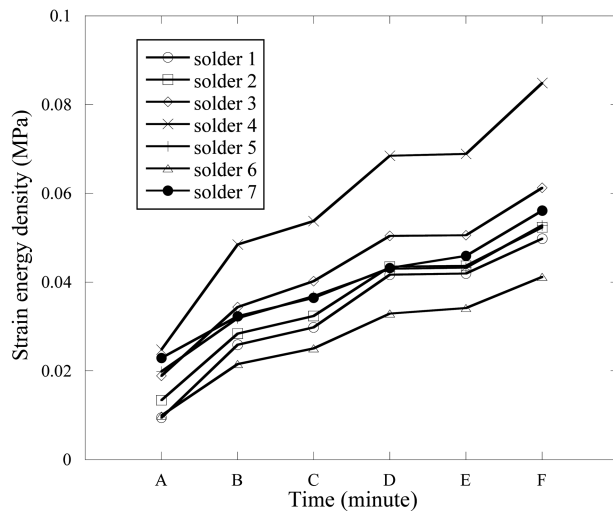
Factor	Type	Level 1	Level 2	Level 3
A	Molding compound thickness	0.25	0.4	0.55
B	PCB thickness	1	1.2	1.4
C	Substrate thickness	0.1	0.2	0.3
D	Solder ball height	0.35	0.4	0.45
E	UBM diameter	0.35	0.45	0.55
F	Solder joint pitch	0.85	1	1.15

Table 3. Noise experiments.

EXp	Factors and levels						W(Mpa)
	A	B	C	D	E	F	
1	1	1	1	1	1	1	0.0805
2	1	1	1	2	2	2	0.0866
3	1	2	2	1	1	2	0.0889
4	1	2	2	2	2	1	0.0767
5	2	1	2	1	2	1	0.0791
6	2	1	2	2	1	2	0.0896
7	2	2	1	1	2	2	0.0935
8	2	2	1	2	1	1	0.0861

Table 4. Results of the noise experiments

Level	A	B	C	D	E	F
1	0.08318	0.08395	0.08668	0.0855	0.08628	0.0806
2	0.08708	0.0863	0.08358	0.08475	0.08398	0.08965
Effect	0.0039	0.00235	0.0031	0.00075	0.0023	0.00905
Rank	2	4	3	6	5	1

**Fig. 6.** Strain energy density accumulations of the original packaging structure under the thermal cycles.

defined as the average of W of factor j at level i . Table 4 and Fig.7 show that solder joint pitch was the most effective noise factor. Therefore, we defined three sets of artificial

Table 5. Results of main experiments.

S/N	Factors and levels									S/N
	A	B	C	D	E	F	N1	N2	N3	
1	1	1	1	1	1	1	0.0982	0.103	0.108	19.7311
2	1	1	1	1	2	2	0.0915	0.095	0.0985	20.4416
3	1	1	1	1	3	3	0.117	0.12	0.124	18.3898
4	1	2	2	2	1	1	0.0702	0.0737	0.0773	22.64
5	1	2	2	2	2	2	0.0684	0.0709	0.0735	22.9793
6	1	2	2	2	3	3	0.084	0.0864	0.0887	21.2709
7	1	3	3	3	1	1	0.0641	0.0676	0.0712	23.3888
8	1	3	3	3	2	2	0.0563	0.0586	0.0609	24.6376
9	1	3	3	3	3	3	0.0616	0.0632	0.0649	23.9791
10	2	1	2	3	1	2	0.101	0.108	0.115	19.3194
11	2	1	2	3	2	3	0.0891	0.0938	0.0986	20.5454
12	2	1	2	3	3	1	0.056	0.0938	0.0593	22.8817
13	2	2	3	1	1	2	0.107	0.114	0.121	18.851
14	2	2	3	1	2	3	0.102	0.107	0.111	19.4343
15	2	2	3	1	3	1	0.0922	0.0927	0.0933	20.6552
16	2	3	1	2	1	2	0.156	0.166	0.177	15.5689
17	2	3	1	2	2	3	0.134	0.142	0.15	16.9451
18	2	3	1	2	3	1	0.0893	0.0913	0.0933	20.7892
19	3	1	3	2	1	3	0.162	0.174	0.187	15.1575
20	3	1	3	2	2	1	0.068	0.0712	0.0746	22.9361
21	3	1	3	2	3	2	0.0834	0.0864	0.0894	21.2662
22	3	2	1	3	1	3	0.232	0.25	0.269	12.0138
23	3	2	1	3	2	1	0.0982	0.104	0.11	19.6445
24	3	2	1	3	3	2	0.094	0.0989	0.104	20.0828
25	3	3	2	1	1	3	0.191	0.206	0.222	13.6923
26	3	3	2	1	2	1	0.0933	0.0965	0.0998	20.3032
27	3	3	2	1	3	2	0.125	0.129	0.134	17.7623

experimental errors to be implemented on the solder ball pitch in the main experiments. For this, same errors of $\pm 4\%$ were applied for each level of the solder joint pitch, which formed the $L_{27} (3^6)$ orthogonal array for the main experiments.

The calculation results based on these errors are listed in



Fig. 7. Responses of noise experiments diagram.

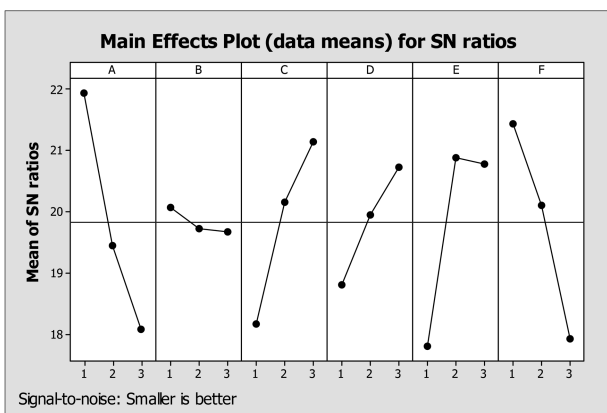


Fig. 8. Responses of main experiments diagram.

Table 5 as N1, N2 and N3. N1 is the accumulated strain energy densities calculated by decreasing the joint pitch by 4%, and N3 by increasing joint pitch by 4%. N2 is for the energy densities that are based on no error. The corresponding S/N values are also listed in Table 5, and plotted in Fig. 8. Through ANOVA, the dominant factors for the optimal design were found to be A (molding compound thickness), C (substrate thickness), E (UBM diameter) and F (solder joint pitch).

Using the results, the optimum packaging structure was constructed and the maximum strain energy density accumulation was calculated again. The calculation results

Table 6. Comparison of the strain energy densities of the original and optimized packaging structures.

Design	Factors and levels						W(Mpa)	S/N
	A	B	C	D	E	F		
Original	2	2	2	2	2	2	0.0849	21.12
Optimal	1	2	3	3	2	1	0.0497	26.72
							41.5%	26.5%

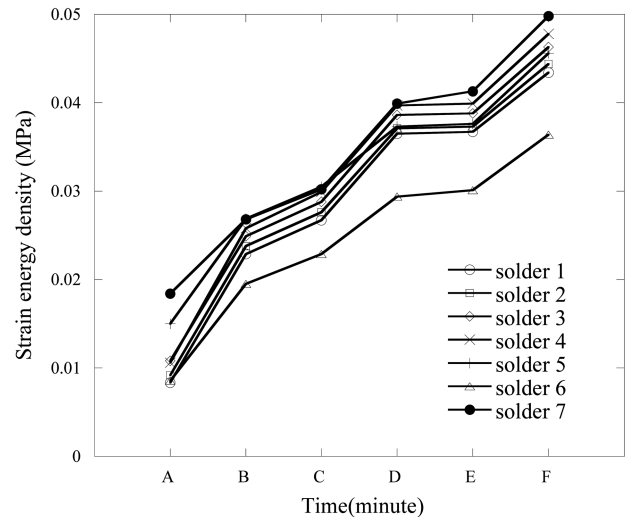


Fig. 9. Strain energy density accumulations of the optimized packaging structure under the thermal cycles.

are shown in Table 6, and compared with the value based on the original packaging structure. It was found that the maximum strain energy density accumulated at the thermal point F (see Fig. 5) based on the optimized dimensions was 0.0497 MPa, which is 41.5% less than the value before the optimization. The S/N ratio was also increased about 26.5%. Fig. 9 represents the strain energy density accumulations of the individual solder balls using the optimized structure. Unlike the original results in Fig. 6, the absolute values of the strain energy densities and their differences among the individual solder balls are noticeably smaller, and the maximum value was found in the no. 7 solder ball which was at the outmost location from the geometric center line ($x=0$).

3. Conclusions

In this study, the Taguchi method was successfully applied to obtain the optimized geometry for the BGA packaging structure. In this level of the structural modeling, the solder ball pitch was found to be the most effective noise factor. By applying the artificial noise to the factors, the main experiments were performed to achieve the minimum strain energy density accumulation. It was found that the maximum strain energy density based on the optimized geometry was about 40% less than that of the original packaging configuration. It was also found that the solder location of the maximum strain energy density was changed from the no. 4 solder ball to the no. 7 solder ball. Actual attempts to change the packaging dimensions such as solder ball pitches, the thicknesses of the molding compound and the substrate may

need careful consideration in the industrial process application. However, this study clearly demonstrates that the effects of the packaging geometry variations on the solder ball reliability are remarkable. The analyses of the differences between the elastic and viscoelastic approaches to account for the viscoelastic behaviors of the materials as control factors are in progress.

References

1. H. Son, I. Kim, S. Lee, K. Jung, B. Park and K. Baik, "Reliability Studies on Cu/SnAg Double-Bump Flip Chip Assemblies for Fine Pitch Applications", *J. Microelectron. Packag. Soc.*, 15(2), 37 (2008).
2. S. Han, I. Cho and Y. Shin, "Reliability of Sn-8Zn-3Bi Solder Paste Applied to Lead and Lead-free Plating on Lead-frame under Thermal Shock Test", *J. Microelectron. Packag. Soc.*, 14(2), 35 (2007).
3. Y. K. Kim, I. S. Park and J. Choi, "Strip type panel warpage analyses for PBGA chip packaging", *Microelectronics Reliability*, 50, 398 (2010).
4. C. Mao and R. Chen, "Packaging parameter analysis and optimization design on solder joint reliability for twin die stacked packages by variance in strain energy density (SED) of each solder joint", *Microelectronics Reliability*, 48, 119 (2008).
5. T. Tee and Z. Zhong, "Board level solder joint reliability analysis and optimization of pyramidal stacked die BGA packages", *Microelectronics Reliability*, 44, 1957 (2004).
6. Y. Lai and T. H. Wang, "Optimal design towards enhancement of board-level thermomechanical reliability of wafer-level chip-scale packages", *Microelectronics Reliability*, 47, 104 (2007).
7. Y. Lai, T. H. Wang and C. Wang, "Optimization of Thermomechanical Reliability of Board-level Package-on-Package Stacking Assembly", *IEEE TRANSACTIONS ON COMPONENTS AND PACKAGING TECHNOLOGIES*, 29, 864 (2006).
8. T. Wang and Y. Lai, "Optimization of Thermomechanical Reliability of Board-Level Flip-Chip Packages Implemented With Organic or Silicon Substrates", *IEEE TRANSACTIONS ON ELECTRONICS PACKAGING MANUFACTURING*, 31(2), 174 (2008).
9. T. Wang, Y. Lai, C. Lee, and Y. Lin, "Coupled Power and Thermal Cycling Reliability of Board-Level Package-on-Package Stacking Assembly", *IEEE TRANSACTIONS ON ELECTRONICS PACKAGING MANUFACTURING*, 32(1), 14 (2009).
10. T. Wang, C. Wang, Y. Lai, K. Chang and C. Lee, "Optimization of board-level thermomechanical reliability of high performance flip-chip package assembly", *Microelectronic Engineering*, 85(4), 659 (2008).
11. G. Taguchi, "Quality engineering (Taguchi methods) for the development of electronic circuit technology", *IEEE Trans Reliab.*, 44(2), 225 (1995).
12. I. Ward and D. Hardley, *An Introduction to the Mechanical Properties of Solid Polymers*, John Wiley & Sons Ltd., United Kingdom (1993).
13. G. Wang, Z. Cheng, K. Becker and J. Wilde, "Applying Anand Model to Represent the Viscoplastic Deformation Behavior of Solder Alloys," *Journal of Electronics Packaging*, 123, 247 (2001).